

1 **Development of a Rapid Point-Of-Care Test that Measures Neutralizing Antibodies**
2 **to SARS-CoV-2**

3 Douglas F. Lake^{1*#}, Alexa J. Roeder^{1*}, Erin Kaleta², Paniz Jasbi³, Kirsten Pfeffer¹,
4 Calvin Koelbel¹ Sivakumar Periasamy^{4,5} Natalia Kuzmina^{4,5} Alexander Bukreyev^{4,5,6},
5 Thomas E. Grys², Liang Wu⁷, John R Mills⁷, Kathrine McAulay², Maria Gonzalez-Moa⁸,
6 Alim Seit-Nebi⁸, and Sergei Svarovsky⁸

7
8 Affiliations:

- 9 1. School of Life Sciences, Arizona State University, Tempe AZ, USA
10 2. Mayo Clinic Arizona, Department of Laboratory Medicine and Pathology,
11 Scottsdale, AZ, USA
12 3. College of Health Solutions, Arizona State University, Phoenix AZ, USA
13 4. Department of Pathology, University of Texas Medical Branch at Galveston,
14 Galveston, TX USA
15 5. Galveston National Laboratory, University of Texas Medical Branch at Galveston,
16 Galveston, TX USA
17 6. Department of Microbiology and Immunology University of Texas Medical Branch
18 at Galveston, Galveston, TX USA
19 7. Mayo Clinic Rochester, Department of Laboratory Medicine and Pathology,
20 Rochester, MN USA
21 8. Axim Biotechnologies Inc, San Diego, CA USA

22 *Co-first authors

23

24 #Address correspondence to Douglas F. Lake, douglas.lake@asu.edu

25

26 Word Count: 2498

27

28 **Abstract:**

29 **Background:** After receiving a COVID-19 vaccine, most recipients want to know if they
30 are protected from infection and for how long. Since neutralizing antibodies are a
31 correlate of protection, we developed a lateral flow assay (LFA) that measures levels of
32 neutralizing antibodies from a drop of blood. The LFA is based on the principle that
33 neutralizing antibodies block binding of the receptor-binding domain (RBD) to
34 angiotensin-converting enzyme 2 (ACE2).

35 **Methods:** The ability of the LFA was assessed to correctly measure neutralization of
36 sera, plasma or whole blood from patients with COVID-19 using SARS-CoV-2
37 microneutralization assays. We also determined if the LFA distinguished patients with
38 seasonal respiratory viruses from patients with COVID-19. To demonstrate the
39 usefulness of the LFA, we tested previously infected and non-infected COVID-19
40 vaccine recipients at baseline and after first and second vaccine doses.

41 **Results:** The LFA compared favorably with SARS-CoV-2 microneutralization assays
42 with an area under the ROC curve of 98%. Sera obtained from patients with seasonal
43 coronaviruses did not show neutralizing activity in the LFA. After a single mRNA
44 vaccine dose, 87% of previously infected individuals demonstrated high levels of
45 neutralizing antibodies. However, if individuals were not previously infected only 24%
46 demonstrated high levels of neutralizing antibodies after one vaccine dose. A second
47 dose boosted neutralizing antibody levels just 8% higher in previously infected
48 individuals, but over 63% higher in non-infected individuals.

49 **Conclusions:** A rapid, semi-quantitative, highly portable and inexpensive neutralizing
50 antibody test might be useful for monitoring rise and fall in vaccine-induced neutralizing
51 antibodies to COVID-19.

52

53 **KEYWORDS**

54 Neutralizing Antibodies, COVID-19, SARS-CoV-2, Lateral Flow Assay, RBD, ACE2

55 INTRODUCTION

56 Severe Acute Respiratory Syndrome Coronavirus-2 (SARS-CoV-2) causes
57 COVID-19 and originated in Wuhan, China in December 2019 [1–3]. Vaccines continue
58 to be tested [4,5] with the goal of preventing COVID-19 via induction of neutralizing
59 antibodies (NAbs) and anti-viral T cells. Vaccine trials show that RNA vaccines elicit
60 protective immunity, but durability of natural and vaccine-induced immunity is not fully
61 known [5]. Several groups reported that up to one-third of serum samples from
62 individuals who recovered from COVID-19 do not neutralize SARS-CoV-2 [6–8].
63 Whether previously infected or vaccinated, it is informative for individuals to learn if they
64 generated high levels of NAbs so that they can resume normal activities without fear of
65 re-infection and transmitting the virus [9–11].

66 Viral neutralization assays measure antibodies that block infection of host cells.
67 The gold standard of neutralization for SARS-CoV-2 measures reduction of viral
68 plaques or foci in microneutralization assays. These assays are slow, laborious, require
69 highly trained personnel and a BSL3 facility. Another challenge is that neutralization
70 assays require careful titration of virus and depend on host cells for infection, both of
71 which add variability to the assay. These limitations prevent use of SARS-CoV-2
72 neutralization assays for clinical applications.

73 SARS-CoV-2 uses receptor binding domain (RBD) on spike protein to bind
74 angiotensin converting enzyme 2 (ACE2) on host cells; RBD appears to be the principal
75 neutralizing domain [12,13]. Using this knowledge, we developed a lateral flow assay
76 (LFA) that measures levels of NAbs which block RBD from binding to ACE2. Other
77 groups have developed RBD-ACE2-based competition ELISAs[18,19] but none have

78 developed a rapid, highly portable, semi-quantitative test that can easily be incorporated
79 into clinical settings or research studies where traditional laboratory or neutralization
80 tests are not practical.

81

82 MATERIALS AND METHODS

83 *Human Subjects and Samples*

84 Serum and finger-stick blood samples were collected for this study under an
85 Arizona State University institutional review board (IRB)-approved protocol
86 #0601000548 and Mayo Clinic IRB protocol #20-004544. Serum samples obtained
87 from excess clinical samples at Mayo Clinic were left over from normal workflow.
88 COVID-19 samples ranged from 3 to 84 days post PCR positive result.

89 Twenty-seven control serum samples from patients with non-COVID-19
90 respiratory illnesses as determined by the FilmArray Respiratory Panel 2 (Biofire
91 Diagnostics) were collected from patients from 2/14/17 – 4/6/20 as part of routine
92 clinical workflow. All residual clinical samples were stored at 2-8°C for up to 7 days, and
93 frozen at -80°C thereafter.

94

95 *SARS-CoV-2 Microneutralization Assay*

96 A microneutralization assay was performed using a recombinant SARS-CoV-2
97 expressing mNeonGreen (SARS-CoV-2ng) as previously described [16]. Inhibitory
98 concentrations for which 50% of virus is neutralized by serum antibodies (IC₅₀ values)
99 were obtained on a set of 38 COVID-19 sera. Sixty µl aliquots of SARS-CoV-2ng were
100 pre-incubated for 1 h in 5% CO₂ at 37°C with 60µl 2-fold serum dilutions in cell culture

101 media, and 100 μ l were inoculated onto Vero-E6 monolayers in black polystyrene 96-
102 well plates with clear bottoms (Corning) in duplicate. The final amount of the virus was
103 200 PFU/well, the starting serum dilution was 1:20 and the end dilution was 1:1280
104 unless an IC₅₀ was not reached in which case serum was diluted to 1:10240. Cells were
105 maintained in Minimal Essential Medium (ThermoFisher Scientific) supplemented by 2%
106 FBS (HyClone) and 0.1% gentamycin in 5% CO₂ at 37°C. After 2 days of incubation,
107 fluorescence intensity of infected cells was measured at 488 nm using a Synergy 2 Cell
108 Imaging Reader (Biotek). Signal was normalized to virus alone with no serum added
109 and reported as percent neutralization. IC₅₀ was calculated with GraphPad Prism 6.0
110 software. Work was performed in a BSL-3 biocontainment laboratory of the University of
111 Texas Medical Branch, Galveston, TX.

112

113 *Serologic Antibody Assay*

114 The Ortho Vitros Anti-SARS-CoV-2 IgG test (Ortho Vitros test) was performed on
115 an Ortho Clinical Diagnostics Vitros 3600 Immunodiagnosics System at the Mayo
116 Clinic. This assay is approved for clinical testing under FDA Emergency Use
117 Authorization to qualitatively detect antibody to the S1 subunit of SARS-CoV-2 spike
118 protein. Results are reported as reactive (S/CO \geq 1.0) or nonreactive (S/CO $<$ 1.0).
119 Specimens were tested within 7 days of collection and stored at 2-8°C. The same 38
120 serum samples were run in the Ortho Vitros test, microneutralization assay, and the
121 LFA.

122

123

124 *Lateral Flow Neutralizing Antibody Assay*

125 The Lateral Flow NAb assay was developed to measure levels of antibodies that
126 compete with ACE2 for binding to RBD. The LFA single port cassette (Empowered
127 Diagnostics) contains a test strip composed of a sample pad, blood filter, conjugate pad,
128 nitrocellulose membrane striped with test and control lines, and an absorbent pad (Axim
129 Biotechnologies Inc). The LFA also contains a control mouse antibody conjugated to
130 red gold nanospheres and corresponding anti-mouse IgG striped at the control line.

131 LFAs were run at room temperature on a flat surface for 10 minutes prior to
132 reading results. To perform the test, 6.7µl of serum or 10ul whole blood were added to
133 the sample port followed by 60µl of chase buffer. After 10 minutes, densities of both test
134 and control lines were recorded in an iDetekt RDS-2500 density reader.

135 The test leverages the interaction between RBD-conjugated green-gold
136 nanoshells (Nanocomposix) that bind ACE2 at the test line when RBD-neutralizing
137 antibodies (RBD-NAbs) are absent or low. Test line density is inversely proportional to
138 RBD-NAbs present within the sample. As a semi-quantitative test, the results of the LFA
139 can be interpreted using a scorecard or a densitometer. A red line across from the “C”
140 indicates that the test ran properly. An absent or faint test line indicates high levels of
141 RBD-NAbs, whereas a dark test line suggests low or lack of RBD-NAbs.

142

143 Precision testing was performed using sera from one highly, and one non-
144 neutralizing donor in replicates of 10. Density values were recorded as above
145 and %CVs calculated using the formula: (Standard Deviation/Mean) * 100%.

146

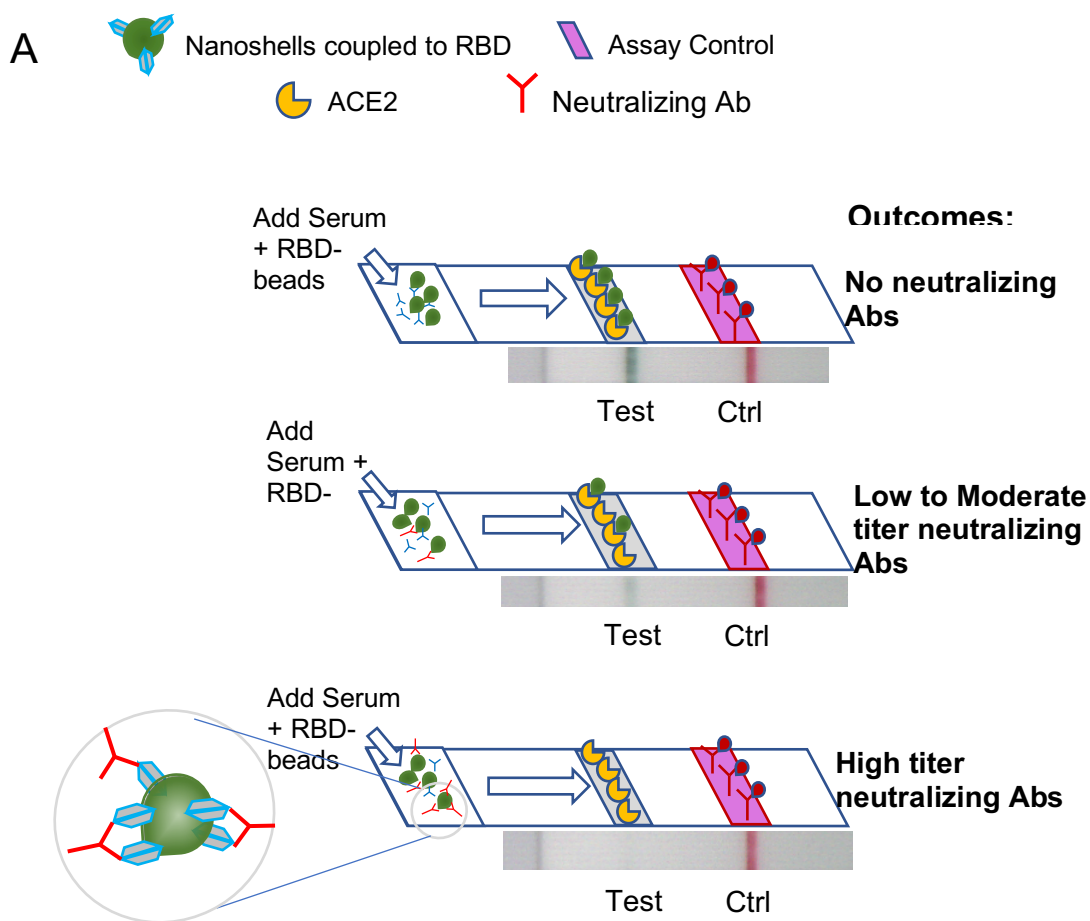
147 *Data Analysis*

148 Pearson's correlation (r) was conducted to assess the strength and significance of
149 associations between the LFA, the Ortho Vitros test and IC_{50} values. Regression analysis
150 using IC_{50} values evaluated consistency [14] while Bland-Altman plots assessed
151 agreement and bias [17,18]. Correlation analysis was conducted using IBM SPSS. For
152 two-group analysis, IC_{50} values corresponding to >240 were categorized as titer of $\geq 1:320$
153 (neutralizing), whereas IC_{50} values ≤ 240 were categorized as $\leq 1:160$ (low/non-
154 neutralizing). Receiver operating characteristic (ROC) analysis was performed to assess
155 accuracy, sensitivity, and specificity of the LFA and Ortho Vitros tests in assessing
156 neutralization; optimal cutoffs for each method were established to maximize area under
157 curve (AUC) [19,20]. ROC analysis was conducted using R language in the RStudio
158 environment (version 3.6.2; RStudio PBC). All analyses were conducted using raw values;
159 data were not normalized, transformed, or scaled.

160

161 RESULTS

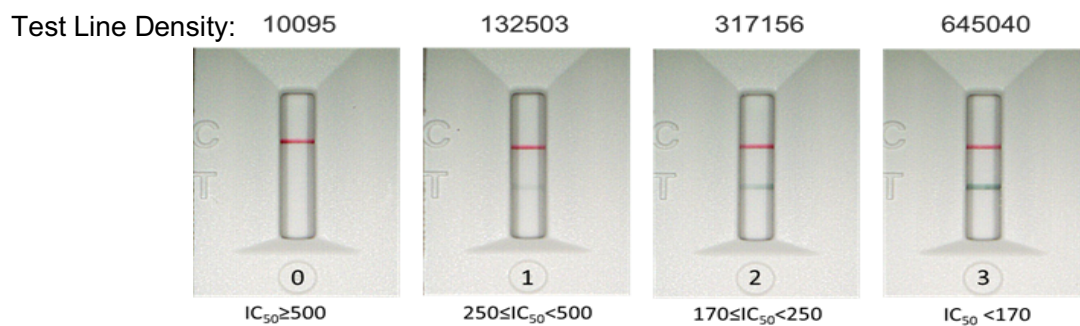
162 As shown at the bottom in **Figure 1A**, serum containing high levels of NAbs
163 results in a weak or ghost test line because NAbs bind RBD on green-gold beads,
164 preventing RBD from binding to the ACE2 receptor at the test line. Serum with low
165 levels of NAbs results in a strong test line because little to no antibodies prevent RBD
166 on beads from binding to ACE2. **Figure 1B** demonstrates results of the test using
167 COVID-19 sera with different levels of NAbs.



168

B

169

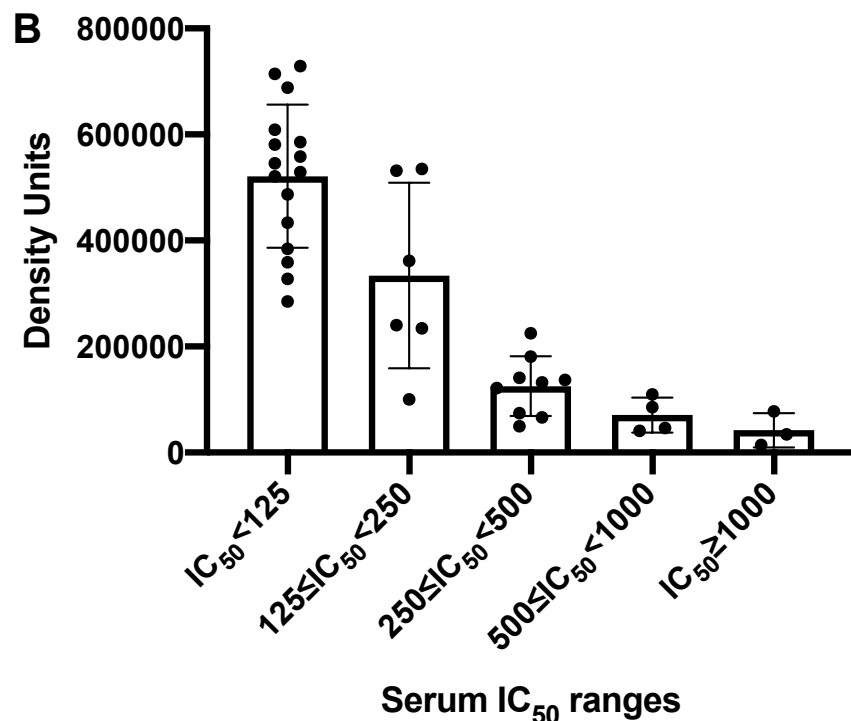


170 **Figure 1. (A)** Schematic of Neutralization LFA. Below each graphic is a representative
171 image of a lateral flow strip demonstrating actual line density. Addition of non-
172 COVID19-immune serum or plasma (*top*) does not block binding of RBD-beads (green
173 particles) to ACE2 resulting in the RBD-bead–ACE2 complex creating a visible line.
174 Addition of patient serum with moderate titer NABs to the sample pad creates a weak
175 line (*middle*). Addition of patient serum with high titer NABs ($> 1:640$) blocks binding of

176 RBD-beads to ACE2 such that no line is observed at the test location on the strip
177 (*bottom*). Red control line represents capture of a mouse monoclonal antibody coupled
178 to red beads. **(B)** Scorecard for measuring levels of NAb. Red control line across
179 from the “C” on the cassette indicates that the test ran properly and the green test line
180 across from the “T” can be used to measure the ability of plasma or serum to block RBD
181 on gold nanoshells from binding to ACE2. **(0)** represents patient serum producing a
182 visually non-existent line with density units of 10,095 and an $IC_{50} > 500$ ($IC_{50} = 1151$); **(1)**
183 represents patient serum with a line density of 132,503 and an IC_{50} of 396; **(2)**
184 represents patient serum with a line density of 239,987 and an IC_{50} of 243; **(3)**
185 represents patient serum with a line density of 485,665 and an IC_{50} of 96.

186

187 To support the application of the LFA to measure NAb levels to SARS-CoV-2, we
188 tested 38 serum samples that were assigned IC_{50} values in a SARS-CoV-2
189 microneutralization assay [16]. The experiment was performed in a blinded manner
190 such that personnel running either the LFA or the microneutralization assay did not
191 know the results of the comparator test. When line densities from the LFA were plotted
192 against IC_{50} values determined in the microneutralization assay, serum samples with
193 strong neutralization activity demonstrated low line densities; this indicates that NAb
194 inhibited RBD from binding to ACE2 (**Figure 2**).



195

196 **Figure 2.** Comparison of RBD-ACE2 competition LFA density values with IC₅₀ values
197 determined in a SARS-CoV-2 microneutralization assay on 38 samples (collected 3 to
198 90 days after PCR positive result). Ranges of IC₅₀ values are shown on the X-axis
199 plotted against LFA line density units on the Y-axis.

200

201

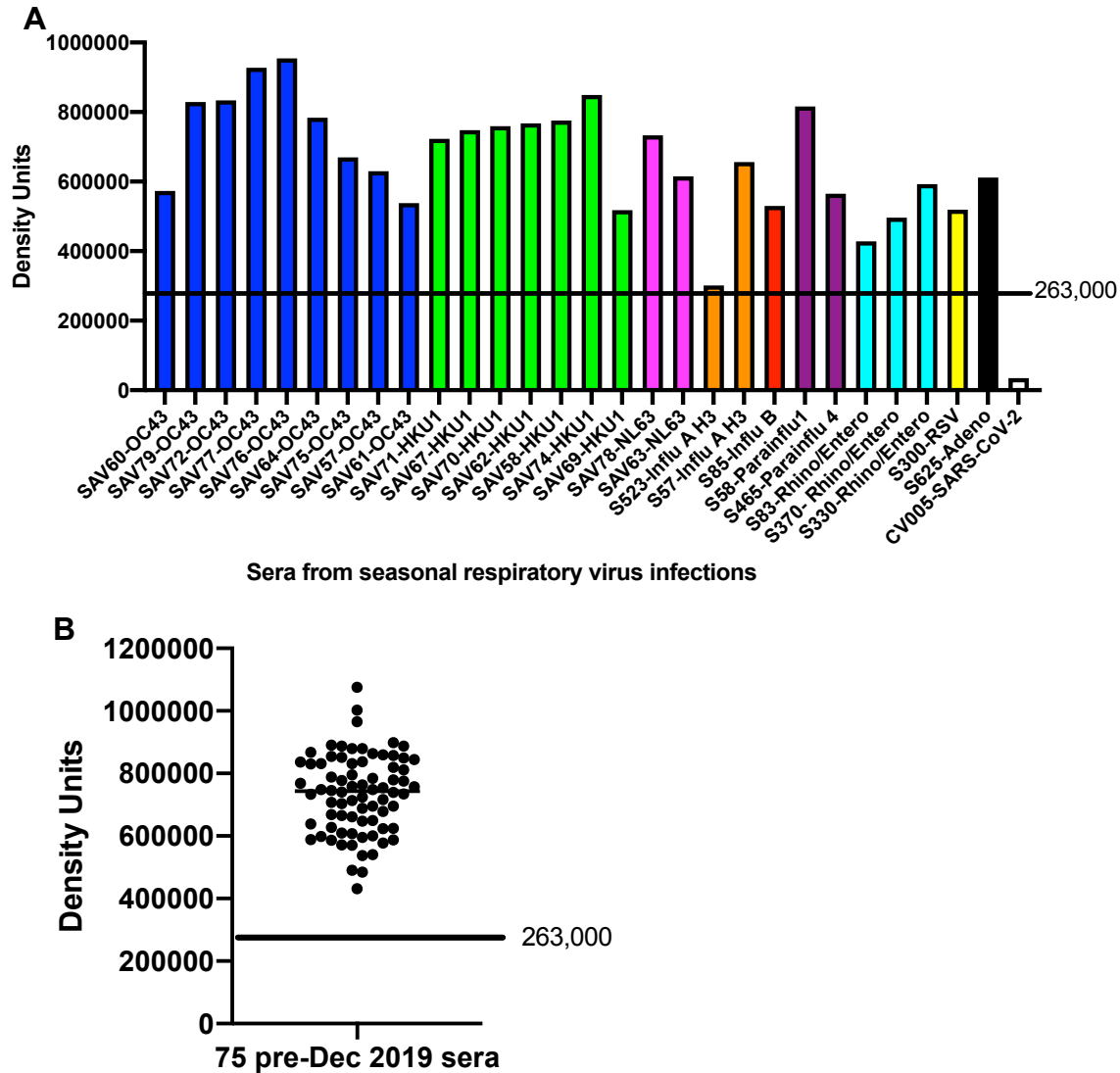
202

203 Next, we determined if the LFA detected neutralization activity in serum samples

204 collected from patients with other PCR-confirmed respiratory viruses including seasonal

205 coronaviruses (**Figure 3A**) and for serum samples collected prior to December 2019

206 (**Figure 3B**). Neither seasonal respiratory virus sera, nor pre-December 2019 samples
showed neutralizing activity.



207

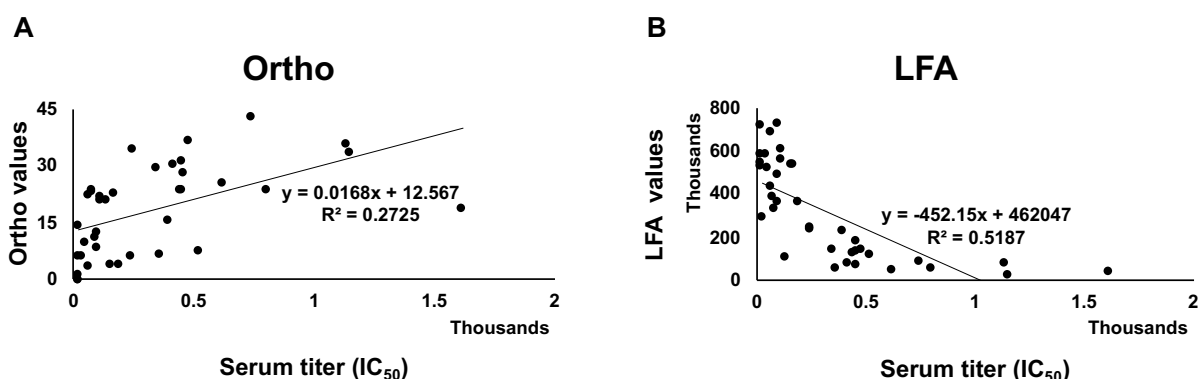
208 **Figure 3. A)** Serum samples collected with PCR-confirmed diagnosis of seasonal
 209 respiratory viruses (Coronavirus OC43, blue; Coronavirus HKU-1, green; Coronavirus
 210 NL-63, pink; influenza A, orange, influenza B, red ; parainfluenza, purple ; rhinovirus,
 211 teal ; respiratory syncycial virus, yellow ; and adenovirus, black were run on the LFA as
 212 described in Methods. A positive control serum from a convalescent COVID-19 patient
 213 is shown on the far right of the bar graph in white. **B)** Serum samples collected pre-
 214 December 2019. Cutoff value of 263,000 density units was calculated based on
 215 receiver operating characteristic curves (see Figure 6).

216

217 We then compared both the Ortho Vitros test and our LFA to sera with IC₅₀ values
218 determined in the SARS-CoV-2 microneutralization assay using 38 COVID-19 sera. To
219 assess agreement between our LFA and the Ortho Vitros test, density units from the LFA
220 and values from the Ortho test were regressed onto IC₅₀ values (**Supplemental Figure**
221 **S1**).

222

223



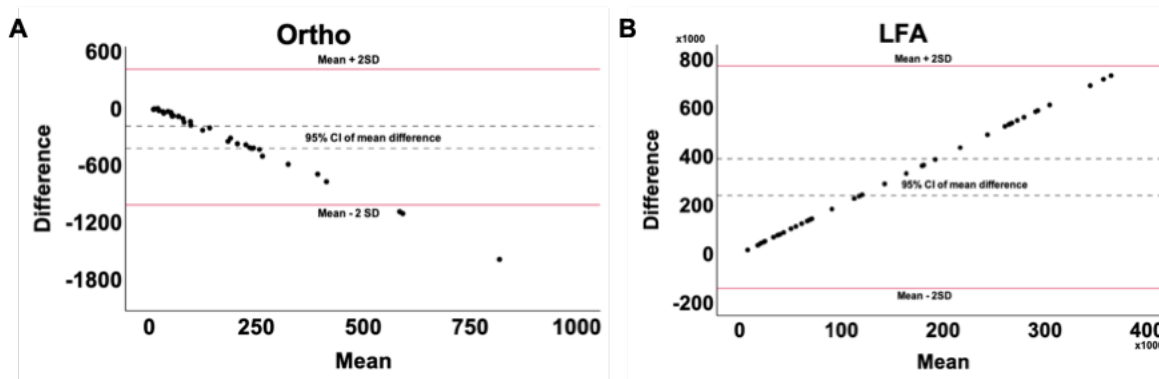
224 **Supplemental Figure S1.** Regression analysis between (A) LFA and serum titer, and
225 (B) Ortho Vitros SARS-CoV-2 IgG test and titer. Regression plots show explained
226 variance (R^2) between compared methods. Thirty-eight samples were tested.
227

228

229 LFA values accounted for roughly 52% of observed variance in IC₅₀ values, while
230 the Ortho Vitros test accounted for approximately 27% of IC₅₀ variance. LFA showed
231 significant negative correlation with IC₅₀ values ($r = -0.720$, $p < 0.001$), while the Ortho
232 Vitros test values showed a significant positive correlation to IC₅₀ values ($r = 0.522$, $p =$
233 0.001). Additionally, the LFA and Ortho Vitros test values correlated with each other ($r =$
234 -0.572 , $p < 0.001$).

235 To evaluate bias, mean differences and 95% confidence intervals (CIs) were
236 calculated and plotted alongside limits of agreement (**Figure 4**). Both LFA and Ortho

237 Vitros test values showed strong agreement with titer, although the Ortho Vitros test
238 showed a tendency to underestimate neutralizing capacity while the LFA method showed
239 no bias.
240



241
242 **Figure 4.** Bland-Altman plots showing bias (mean difference and 95% CI) and
243 computed limits of agreement (mean difference \pm 2SD) between **(A)** Ortho Vitros Anti-
244 SARS-CoV-2 IgG test and IC₅₀ values and **(B)** our LFA and IC₅₀ values. Thirty-eight
245 samples were tested.

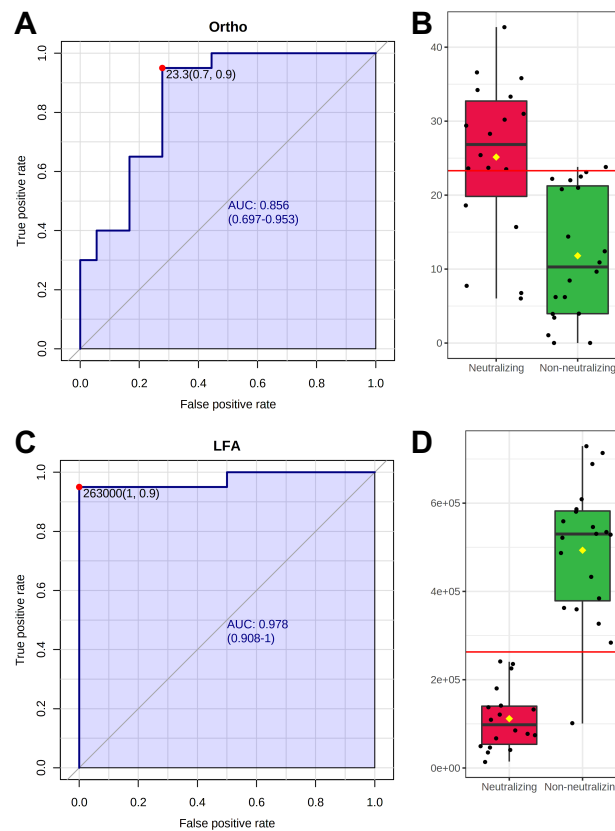
246
247
248 ROC analysis was performed to assess the ability of the LFA and the Ortho Vitros
249 test to classify low/non-neutralizing (Neg, <1:160), and highly neutralizing groups (\geq 1:320)
250 **(Figure 5)**. As shown in **Figure 5B** and **5D**, the LFA misclassified one non-neutralizing
251 sample (Neg, <1:160) as neutralizing (\geq 1:320) which the Ortho Vitros test also
252 misclassified as neutralizing. The Ortho test also incorrectly classified five additional
253 neutralizing samples as non-neutralizing.

254 Our LFA showed high accuracy for classification of neutralizing samples (AUC =
255 0.978), while the Ortho Vitros test showed modest accuracy (AUC = 0.856). Notably, while
256 both methods showed roughly 90% sensitivity, the Ortho Vitros test showed only 70%

257 specificity. In contrast, the LFA showed perfect specificity (100%) in this analysis of 38
258 samples.

259 Optimal cutoffs were computed to maximize AUC. For the LFA, density unit values
260 below 263,000 classify samples as neutralizing and correspond to titers $\geq 1:320$. Density
261 values above this LFA cutoff classify samples in the non-neutralizing group. For the Ortho
262 Vitros test, values between 0 and 23.3 were representative of non-neutralizing capacity,
263 whereas values above 23.3 were reflective of the neutralizing group.

264



265 **Figure 5. (A)** Univariate ROC analysis of Ortho Vitros Anti-SARS-CoV-2 IgG test for
 266 discrimination of neutralizing samples ($\geq 1:320$) [AUC: 0.856, 95% CI: 0.697—0.953,
 267 sensitivity = 0.9, specificity = 0.7]. **(B)** Box plot of Ortho Vitros Anti-SARS-CoV-2 IgG test
 268 values between neutralizing ($\geq 1:320$) and non-neutralizing (Neg—1:160) groups. **(C)**
 269 Univariate ROC analysis of LFA for discrimination of neutralizing samples ($\geq 1:320$) [AUC:
 270 0.978, 95% CI: 0.908—1.0, sensitivity = 0.9, specificity = 1.0]. **(D)** Box plot of LFA values
 271 between neutralizing ($\geq 1:320$) and non-neutralizing (Neg—1:160) groups.

272
 273 Precision studies were performed on replicate samples (n=10) and showed a CV
 274 of ~9% from a serum sample in the high neutralizing range and ~6% CV in a serum
 275 sample from the low neutralizing range (Supplemental Table 1).

276

Low Neutralizing Range			
10 min	C	T	T/C Ratio at 10 min
1	503764	932173	1.850416068
2	484316	944154	1.949458618
3	509424	902070	1.770764628
4	441318	840951	1.905544301
5	484558	990076	2.043255916
6	472319	906922	1.920147189
7	519936	971429	1.868362645
8	495254	992223	2.00346287
9	467545	816303	1.745934616
10	534262	941643	1.762511652
Average	491269.6	923794.4	1.88198585
STD Dev	25849.98843	55966.17114	0.096780674
%CV	5.26	6.06	5.14

High Neutralizing Range			
10 min	C	T	T/C Ratio at 10 min
1	415421	232022	0.558522559
2	404845	286183	0.706895232
3	419873	261146	0.621964261
4	417475	248141	0.594385293
5	409970	263808	0.64348123
6	397812	294120	0.739344213
7	409681	237096	0.578733209
8	412275	242082	0.587185738
9	373751	222959	0.596544223
10	373339	224335	0.600888201
Average	403444.2	251189.2	0.622794416
STD Dev	16097.74032	23457.01668	0.055137744
%CV	3.99	9.34	8.85

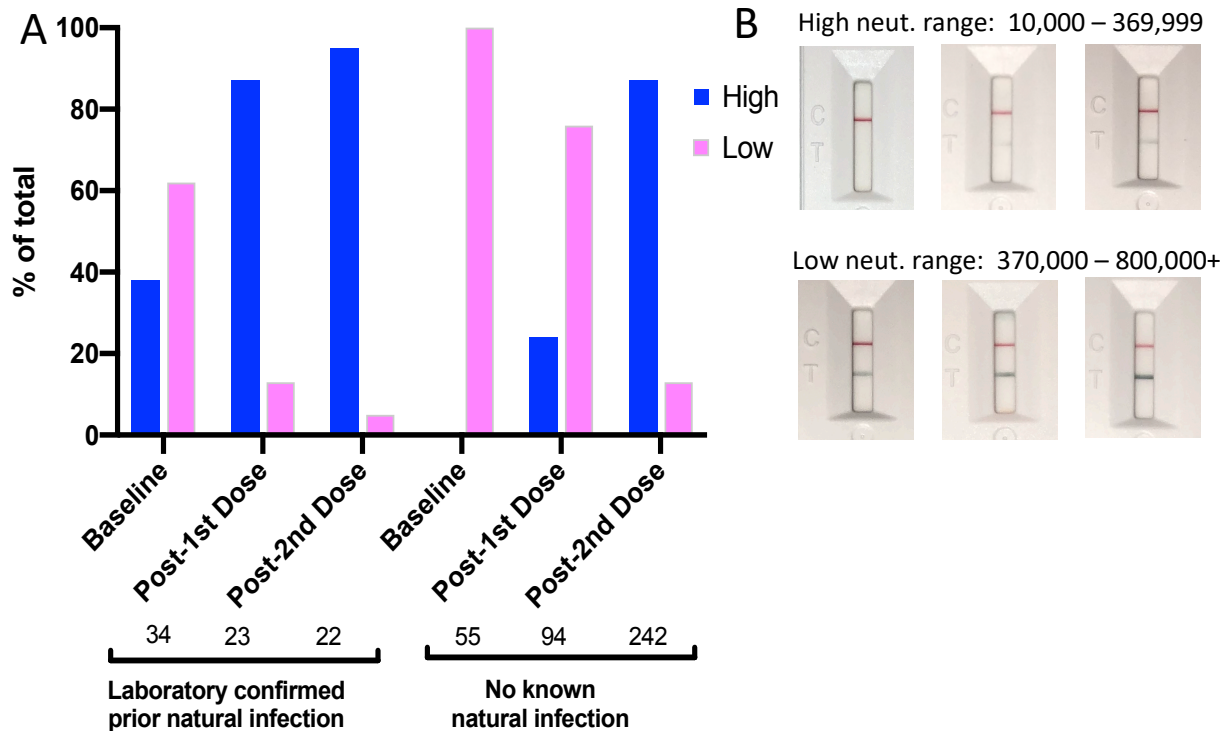
277

278 **Supplemental Table 1.** Precision study using one Low Neutralizing Range serum
 279 sample and one High Neutralizing Range serum sample in replicates of ten. Low range
 280 neutralization is defined as densities from 370,000 – 800,000. The used for precision
 281 analysis was from an individual who recovered from COVID-19 but did not neutralize
 282 virus in the microneutralization assay ($IC_{50} < 20$). High neutralization range samples are
 283 defined as densities from 10,000 – 369,999. This sample has an IC_{50} of 248.

284

285 Precision studies were performed on replicate samples (n=10) and showed a CV
 286 of ~9% from a serum sample in the high neutralizing range and ~6% CV in a serum
 287 sample from the low neutralizing range (**Supplemental Table 1**).

288
289 Since NAb levels may be considered correlates of protection, we tested sera
290 from RNA vaccine recipients (mRNA-1723 and BNT162b2) in “previously infected” and
291 “not previously infected” individuals using finger-stick blood in the rapid LFA (**Figure 6**).
292 In *previously infected* individuals at baseline (within 3 months of PCR-based diagnosis),
293 38% demonstrated high levels of NABs. After the first vaccine dose, 87% of *previously*
294 *infected* individuals demonstrated high NAb levels, while only 24% of *not previously*
295 *infected* individuals developed high levels of NABs. After the second vaccine dose,
296 levels of NABs increased to 95% in the *previously infected* cohort, while NAb levels
297 increased to 87% in the *not previously infected* cohort. This data suggests that a
298 second vaccine dose is important for highest levels of NABs.
299



300

301 **Figure 6. NAb levels in prior infection and vaccine-induced individuals. (A)**
302 Baseline indicates within one week of first vaccine dose; Post-1st Dose indicates within
303 one week of 2nd vaccine dose; Post 2nd Dose indicates 10-20 days after 2nd vaccine
304 dose. High and Low indicates density ranges of Test lines shown in (B). Densities were
305 read in a reader as described in Methods. Serum titers that correspond to high range
306 densities are >1:1280 to ≥1:160. Serum titers corresponding to low range densities are
307 <1:160.

308

309 DISCUSSION

310 We developed a rapid test that measures levels of NAbs in serum and whole
311 blood. As shown in **Figure 2**, the LFA correlates well with serologic titers determined
312 using a SARS-CoV-2 microneutralization assay, especially when serum sample IC₅₀
313 values are >250. Advantages of the LFA test are that it can be inexpensively and
314 rapidly deployed to determine levels of NAbs in vaccine recipients. Moreover, the test
315 can be used longitudinally to evaluate duration of protective immunity in naturally
316 infected and vaccinated individuals—many more than could ever be evaluated using
317 BSL2 or BSL3-based neutralization assays.

318

319 The LFA and Ortho Vitros test showed a significant correlation with each other (r
320 = -0.572, $p < 0.001$), displaying good linear relation ($r = -0.720$, $p < 0.001$)[21]. The LFA
321 accounts for 52% of observed IC₅₀ variance ($R^2 = 0.5187$), while the Ortho Vitros test
322 accounts for 27% ($R^2 = 0.2725$). Although absolute quantitation demands an excellent
323 coefficient of determination ($R^2 \geq 0.99$)[22], variables with $R^2 \geq 0.5$ are highly predictive
324 in univariate regression models while measures with $R^2 < 0.5$ are recommended for use
325 in multivariate models with complementary measures to increase predictive accuracy

326 [23,24]. Bland-Altman analysis (**Figure 4**) showed the Ortho Vitros test to be prone to
327 underestimation of IC₅₀ values, while the LFA method did not exhibit over- or
328 underestimation bias. Furthermore, across mean values for both methods, the LFA
329 showed discrete differential values while the Ortho Vitros test struggled to differentiate
330 high neutralizing samples.

331

332 Using our rapid test to measure NABs in previously infected vaccine recipients
333 and those who were not infected agrees with other studies in BSL3 facilities using
334 serum from venipuncture blood [5,25–29]. Natural infection may not elicit high levels of
335 NABs [6–8], but a first dose of vaccine induces high levels of NABs in the majority of
336 recipients similar to 2 doses of vaccine in non-previously infected individuals,
337 suggesting natural infection primes the immune system[30]. In naïve individuals, a
338 single dose of vaccine elicits high NAb levels (Titers >1:160) in only 24% of vaccine
339 recipients, leaving 76% of vaccine recipients with titers lower than 1:160 which would
340 not qualify for convalescent plasma donation according to FDA memo of March 9,2021.
341 After a second vaccine dose, the LFA indicated high levels of NABs in 87% of
342 recipients, identical to levels observed in previously infected individuals after the first
343 vaccine dose. These findings might suggest that a booster (3rd vaccine dose) in non-
344 infected individuals could induce the highest levels of NABs in the most people.

345

346 Limitations of the LFA are that it uses only the RBD portion of spike protein.
347 Although the vast majority of reports indicate that the principle neutralizing domain is the
348 RBD portion of spike protein, mAbs have been reported that neutralize SARS-CoV-2 by

349 binding to the N-terminal domain of spike protein [31,32]. Also, since the spike protein
350 assumes multiple conformations during viral binding and entry [33], neutralizing
351 epitopes exist on the quaternary structure of spike [32]. Although RBDs on the
352 nanoparticles may associate, it is not known if they assume a native conformation.

353 Other limitations are the binary nature of this data analysis (high and low
354 neutralizing) of a continuous assay. NAb levels should be evaluated longitudinally to
355 assess rise and fall in NAb levels; this rapid test is well-suited for that role. Another
356 limitation is that the LFA does not differentiate high affinity anti-RBD NAb from an
357 abundance of lower affinity anti-RBD NAb.

358 This test may prove useful in monitoring COVID-19 vaccine recipients as a
359 correlate of protection. It would be logistically difficult to obtain a tube of blood from
360 every vaccine recipient for BSL3 work. However, since this LFA requires only a drop of
361 blood, individual use of this test might lead to more comprehensive longitudinal
362 monitoring of protective humoral immunity and indicate when boosters might be
363 required.

364
365

366 AUTHOR CONTRIBUTIONS

367 DL, SS and AS-N developed the LFA. AJ performed the experiments and interpreted
368 the results. PJ performed statistical analysis. EK, TG and KM contributed samples.
369 CK, AJ and KP tested vaccine recipients and interpreted results. SP, NK and AB
370 performed SARS-CoV-2 microneutralization assays and interpreted results LW and JM
371 contributed samples for preliminary experiments. MM-G designed the strip layout and
372 produced the strips for the vaccine study.

373

374 CONFLICTS OF INTEREST STATEMENT

375 DL and SS are co-founders of Sapphire, the research division of Axim Biotech. SS, MM-
376 G and AS-N are employees of Axim Biotech. Other authors have no conflicts regarding
377 this work.

378

379 FUNDING

380 This study was funded in part by Axim Biotech, San Diego, CA

381

382 References

- 383 [1] I. Ghinai, T.D. McPherson, J.C. Hunter, H.L. Kirking, D. Christiansen, K. Joshi, R. Rubin, S.
384 Morales-Estrada, S.R. Black, M. Pacilli, M.J. Fricchione, R.K. Chugh, K.A. Walblay, N.S.
385 Ahmed, W.C. Stoecker, N.F. Hasan, D.P. Burdsall, H.E. Reese, M. Wallace, C. Wang, D.
386 Moeller, J. Korpics, S.A. Novosad, I. Benowitz, M.W. Jacobs, V.S. Dasari, M.T. Patel, J.
387 Kauerauf, E.M. Charles, N.O. Ezike, V. Chu, C.M. Midgley, M.A. Rolfes, S.I. Gerber, X. Lu, S.
388 Lindstrom, J.R. Verani, J.E. Layden, S. Brister, K. Goldesberry, S. Hoferka, D. Jovanov, D.
389 Nims, L. Saathoff-Huber, C. Hoskin Snelling, H. Adil, R. Ali, E. Andreychak, K. Bemis, M.
390 Frias, P. Quartey-Kumapley, K. Baskerville, E. Murphy, E. Murskyj, Z. Noffsinger, J. Vercillo,
391 A. Elliott, U.S. Onwuta, D. Burck, G. Abedi, R.M. Burke, R. Fagan, J. Farrar, A.M. Fry, A.J.
392 Hall, A. Haynes, C. Hoff, S. Kamili, M.E. Killerby, L. Kim, S.A. Kujawski, D.T. Kuhar, B. Lynch,
393 L. Malapati, M. Marlow, J.R. Murray, B. Rha, S.K.K. Sakthivel, S.E. Smith-Jeffcoat, E. Soda, L.
394 Wang, B.L. Whitaker, T.M. Uyeki, First known person-to-person transmission of severe
395 acute respiratory syndrome coronavirus 2 (SARS-CoV-2) in the USA, *The Lancet*. 395 (2020)
396 1137–1144. [https://doi.org/10.1016/S0140-6736\(20\)30607-3](https://doi.org/10.1016/S0140-6736(20)30607-3).
- 397 [2] C. Huang, Y. Wang, X. Li, L. Ren, J. Zhao, Y. Hu, L. Zhang, G. Fan, J. Xu, X. Gu, Z. Cheng, T. Yu,
398 J. Xia, Y. Wei, W. Wu, X. Xie, W. Yin, H. Li, M. Liu, Y. Xiao, H. Gao, L. Guo, J. Xie, G. Wang, R.
399 Jiang, Z. Gao, Q. Jin, J. Wang, B. Cao, Clinical features of patients infected with 2019 novel
400 coronavirus in Wuhan, China, *The Lancet*. 395 (2020) 497–506.
401 [https://doi.org/10.1016/S0140-6736\(20\)30183-5](https://doi.org/10.1016/S0140-6736(20)30183-5).
- 402 [3] R. Li, S. Pei, B. Chen, Y. Song, T. Zhang, W. Yang, J. Shaman, Substantial undocumented
403 infection facilitates the rapid dissemination of novel coronavirus (SARS-CoV-2), *Science*.
404 368 (2020) 489–493. <https://doi.org/10.1126/science.abb3221>.
- 405 [4] F.P. Polack, S.J. Thomas, N. Kitchin, J. Absalon, A. Gurtman, S. Lockhart, J.L. Perez, G. Pérez
406 Marc, E.D. Moreira, C. Zerbini, R. Bailey, K.A. Swanson, S. Roychoudhury, K. Koury, P. Li,
407 W.V. Kalina, D. Cooper, R.W. Frenck, L.L. Hammitt, Ö. Türeci, H. Nell, A. Schaefer, S. Ünal,

- 408 D.B. Tresnan, S. Mather, P.R. Dormitzer, U. Şahin, K.U. Jansen, W.C. Gruber, Safety and
409 Efficacy of the BNT162b2 mRNA Covid-19 Vaccine, *N. Engl. J. Med.* 383 (2020) 2603–2615.
410 <https://doi.org/10.1056/NEJMoa2034577>.
- 411 [5] A.T. Widge, N.G. Roupael, L.A. Jackson, E.J. Anderson, P.C. Roberts, M. Makhene, J.D.
412 Chappell, M.R. Denison, L.J. Stevens, A.J. Pruijssers, A.B. McDermott, B. Flach, B.C. Lin, N.A.
413 Doria-Rose, S. O’Dell, S.D. Schmidt, K.M. Neuzil, H. Bennett, B. Leav, M. Makowski, J.
414 Albert, K. Cross, V.-V. Edara, K. Floyd, M.S. Suthar, W. Buchanan, C.J. Luke, J.E.
415 Ledgerwood, J.R. Mascola, B.S. Graham, J.H. Beigel, Durability of Responses after SARS-
416 CoV-2 mRNA-1273 Vaccination, *N Engl J Med.* (2020) 4.
- 417 [6] D.F. Robbiani, C. Gaebler, F. Muecksch, J.C.C. Lorenzi, Z. Wang, A. Cho, M. Agudelo, C.O.
418 Barnes, A. Gazumyan, S. Finkin, T. Hagglof, T.Y. Oliveira, C. Viant, A. Hurley, H.-H.
419 Hoffmann, K.G. Millard, R.G. Kost, M. Cipolla, K. Gordon, F. Bianchini, S.T. Chen, V. Ramos,
420 R. Patel, J. Dizon, I. Shimeliovich, P. Mendoza, H. Hartweger, L. Nogueira, M. Pack, J.
421 Horowitz, F. Schmidt, Y. Weisblum, E. Michailidis, A.W. Ashbrook, E. Waltari, J.E. Pak, K.E.
422 Huey-Tubman, N. Koranda, P.R. Hoffman, A.P. West, C.M. Rice, T. Hatziioannou, P.J.
423 Bjorkman, P.D. Bieniasz, M. Caskey, M.C. Nussenzweig, Convergent Antibody Responses to
424 SARS-CoV-2 Infection in Convalescent Individuals, *Immunology*, 2020.
425 <https://doi.org/10.1101/2020.05.13.092619>.
- 426 [7] J.A. Juno, H.-X. Tan, W.S. Lee, A. Reynaldi, H.G. Kelly, K. Wragg, R. Esterbauer, H.E. Kent, C.J.
427 Batten, F.L. Mordant, N.A. Gherardin, P. Pymm, M.H. Dietrich, N.E. Scott, W.-H. Tham, D.I.
428 Godfrey, K. Subbarao, M.P. Davenport, S.J. Kent, A.K. Wheatley, Immunogenic profile of
429 SARS-CoV-2 spike in individuals recovered from COVID-19, *Infectious Diseases (except*
430 *HIV/AIDS)*, 2020. <https://doi.org/10.1101/2020.05.17.20104869>.
- 431 [8] F. Wu, A. Wang, M. Liu, Q. Wang, J. Chen, S. Xia, Y. Ling, Y. Zhang, J. Xun, L. Lu, S. Jiang, H.
432 Lu, Y. Wen, J. Huang, Neutralizing antibody responses to SARS-CoV-2 in a COVID-19
433 recovered patient cohort and their implications, *MedRxiv Prepr.* (2020) 20.
434 <https://doi.org/10.1101/2020.03.30.20047365>.
- 435 [9] Z. Han, F. Battaglia, S.R. Terlecky, Discharged COVID-19 Patients Testing Positive Again for
436 SARS-CoV-2 RNA: A Minireview of Published Studies from China, *J. Med. Virol.* (2020)
437 *jmv.26250*. <https://doi.org/10.1002/jmv.26250>.
- 438 [10] G. Ye, Z. Pan, Y. Pan, Q. Deng, L. Chen, J. Li, Y. Li, X. Wang, Clinical characteristics of severe
439 acute respiratory syndrome coronavirus 2 reactivation, *J. Infect.* 80 (2020) e14–e17.
440 <https://doi.org/10.1016/j.jinf.2020.03.001>.
- 441 [11] V.T. Hoang, T.L. Dao, P. Gautret, Recurrence of positive SARS-CoV-2 in patients recovered
442 from COVID-19, *J. Med. Virol.* (2020) *jmv.26056*. <https://doi.org/10.1002/jmv.26056>.
- 443 [12] Q. Wang, Y. Zhang, L. Wu, S. Niu, C. Song, Z. Zhang, G. Lu, C. Qiao, Y. Hu, K.-Y. Yuen, Q.
444 Wang, H. Zhou, J. Yan, J. Qi, Structural and Functional Basis of SARS-CoV-2 Entry by Using
445 Human ACE2, *Cell.* (2020) S009286742030338X.
446 <https://doi.org/10.1016/j.cell.2020.03.045>.
- 447 [13] L. Premkumar, B. Segovia-Chumbez, R. Jadi, D.R. Martinez, R. Raut, A. Markmann, C.
448 Cornaby, L. Bartelt, S. Weiss, Y. Park, C.E. Edwards, E. Weimer, E.M. Scherer, N. Roupael,
449 S. Edupuganti, D. Weiskopf, L.V. Tse, Y.J. Hou, D. Margolis, A. Sette, M.H. Collins, J.
450 Schmitz, R.S. Baric, A.M. de Silva, The receptor binding domain of the viral spike protein is

- 451 an immunodominant and highly specific target of antibodies in SARS-CoV-2 patients, *Sci.*
452 *Immunol.* 5 (2020) eabc8413. <https://doi.org/10.1126/sciimmunol.abc8413>.
- 453 [14] C.W. Tan, W.N. Chia, X. Qin, P. Liu, M.I.-C. Chen, C. Tiu, Z. Hu, V.C.-W. Chen, B.E. Young,
454 W.R. Sia, Y.-J. Tan, R. Foo, Y. Yi, D.C. Lye, D.E. Anderson, L.-F. Wang, A SARS-CoV-2
455 surrogate virus neutralization test based on antibody-mediated blockage of ACE2–spike
456 protein–protein interaction, *Nat. Biotechnol.* (2020). [https://doi.org/10.1038/s41587-020-](https://doi.org/10.1038/s41587-020-0631-z)
457 [0631-z](https://doi.org/10.1038/s41587-020-0631-z).
- 458 [15] Q.M. Hanson, K.M. Wilson, M. Shen, Z. Itkin, R.T. Eastman, P. Shinn, M.D. Hall, Targeting
459 ACE2-RBD interaction as a platform for COVID19 therapeutics: Development and drug
460 repurposing screen of an AlphaLISA proximity assay, *Biochemistry*, 2020.
461 <https://doi.org/10.1101/2020.06.16.154708>.
- 462 [16] X. Xie, A. Muruato, K.G. Lokugamage, K. Narayanan, X. Zhang, J. Zou, J. Liu, C. Schindewolf,
463 N.E. Bopp, P.V. Aguilar, K.S. Plante, S.C. Weaver, S. Makino, J.W. LeDuc, V.D. Menachery,
464 P.-Y. Shi, An Infectious cDNA Clone of SARS-CoV-2, *Cell Host Microbe.* 27 (2020) 841-
465 848.e3. <https://doi.org/10.1016/j.chom.2020.04.004>.
- 466 [17] Davide Giavarina, Understanding Bland Altman analysis, *Biochem. Medica.* 25 (2015) 141–
467 151. <https://doi.org/10.11613/BM.2015.015>.
- 468 [18] N.Ö. Doğan, Bland-Altman analysis: A paradigm to understand correlation and agreement,
469 *Turk. J. Emerg. Med.* 18 (2018) 139–141. <https://doi.org/10.1016/j.tjem.2018.09.001>.
- 470 [19] N.A. Obuchowski, J.A. Bullen, Receiver operating characteristic (ROC) curves: review of
471 methods with applications in diagnostic medicine, *Phys Med Biol.* (2018) 29.
- 472 [20] C.T. Nakas, C.T. Yannoutsos, Ordered multiple-class ROC analysis with continuous
473 measurements, *Med. Stat.* 23 (November 30) 3437–49. <https://doi.org/10.1002/sim.1917>.
- 474 [21] P. Schober, C. Boer, L.A. Schwarte, Correlation Coefficients: Appropriate Use and
475 Interpretation, *Anesth. Analg.* 126 (2018) 1763–1768.
476 <https://doi.org/10.1213/ANE.0000000000002864>.
- 477 [22] J.D. Rights, S.K. Sterba, Quantifying explained variance in multilevel models: An integrative
478 framework for defining R-squared measures, *Psychol. Methods.* 24 (n.d.) 309–338.
479 <https://doi.org/10.1037/met0000184>.
- 480 [23] J.D. Rights, S.K. Sterba, A framework of R-squared measures for single-level and multilevel
481 regression mixture models, *Psychol. Methods.* 23 (n.d.) 434–457.
482 <https://doi.org/10.1037/met0000139>.
- 483 [24] J.D. Rights, S.K. Sterba, New Recommendations on the Use of R-Squared Differences in
484 Multilevel Model Comparisons, *Multivar. Behav. Res.* 55 (n.d.) 568–599.
- 485 [25] L.A. Jackson, E.J. Anderson, N.G. Rouphael, P.C. Roberts, M. Makhene, R.N. Coler, M.P.
486 McCullough, J.D. Chappell, M.R. Denison, L.J. Stevens, A.J. Pruijssers, A. McDermott, B.
487 Flach, N.A. Doria-Rose, K.S. Corbett, K.M. Morabito, S. O’Dell, S.D. Schmidt, P.A. Swanson,
488 M. Padilla, J.R. Mascola, K.M. Neuzil, H. Bennett, W. Sun, E. Peters, M. Makowski, J. Albert,
489 K. Cross, W. Buchanan, R. Pikaart-Tautges, J.E. Ledgerwood, B.S. Graham, J.H. Beigel, An
490 mRNA Vaccine against SARS-CoV-2 — Preliminary Report, *N. Engl. J. Med.* 383 (2020)
491 1920–1931. <https://doi.org/10.1056/NEJMoa2022483>.
- 492 [26] A. Lombardi, G. Bozzi, R. Ungaro, S. Villa, V. Castelli, D. Mangioni, A. Muscatello, A. Gori, A.
493 Bandera, Mini Review Immunological Consequences of Immunization With COVID-19

- 494 mRNA Vaccines: Preliminary Results, *Front. Immunol.* 12 (2021) 657711.
495 <https://doi.org/10.3389/fimmu.2021.657711>.
- [27] U. Sahin, A. Muik, E. Derhovanessian, I. Vogler, L.M. Kranz, M. Vormehr, A. Baum, K. Pascal, J. Quandt, D. Maurus, S. Brachtendorf, V. Lörks, J. Sikorski, R. Hilker, D. Becker, A.-K. Eller, J. Grützner, C. Boesler, C. Rosenbaum, M.-C. Kühnle, U. Luxemburger, A. Kemmer-Brück, D. Langer, M. Bexon, S. Bolte, K. Karikó, T. Palanche, B. Fischer, A. Schultz, P.-Y. Shi, C. Fontes-Garfias, J.L. Perez, K.A. Swanson, J. Loschko, I.L. Scully, M. Cutler, W. Kalina, C.A. Kyratsous, D. Cooper, P.R. Dormitzer, K.U. Jansen, Ö. Türeci, COVID-19 vaccine BNT162b1 elicits human antibody and TH1 T cell responses, *Nature*. 586 (2020) 594–599.
503 <https://doi.org/10.1038/s41586-020-2814-7>.
- [28] E.J. Anderson, N.G. Rouphael, A.T. Widge, L.A. Jackson, P.C. Roberts, M. Makhene, J.D. Chappell, M.R. Denison, L.J. Stevens, A.J. Pruijssers, A.B. McDermott, B. Flach, B.C. Lin, N.A. Doria-Rose, S. O’Dell, S.D. Schmidt, K.S. Corbett, P.A. Swanson, M. Padilla, K.M. Neuzil, H. Bennett, B. Leav, M. Makowski, J. Albert, K. Cross, V.V. Edara, K. Floyd, M.S. Suthar, D.R. Martinez, R. Baric, W. Buchanan, C.J. Luke, V.K. Phadke, C.A. Rostad, J.E. Ledgerwood, B.S. Graham, J.H. Beigel, Safety and Immunogenicity of SARS-CoV-2 mRNA-1273 Vaccine in Older Adults, *N. Engl. J. Med.* 383 (2020) 2427–2438.
511 <https://doi.org/10.1056/NEJMoa2028436>.
- [29] N. Doria-Rose, M.S. Suthar, M. Makowski, S. O’Connell, A.B. McDermott, B. Flach, J.E. Ledgerwood, J.R. Mascola, B.S. Graham, B.C. Lin, S. O’Dell, S.D. Schmidt, A.T. Widge, V.-V. Edara, E.J. Anderson, L. Lai, K. Floyd, N.G. Rouphael, V. Zarnitsyna, P.C. Roberts, M. Makhene, W. Buchanan, C.J. Luke, J.H. Beigel, L.A. Jackson, K.M. Neuzil, H. Bennett, B. Leav, J. Albert, P. Kunwar, Antibody Persistence through 6 Months after the Second Dose of mRNA-1273 Vaccine for Covid-19, *N. Engl. J. Med.* (2021) NEJMc2103916.
518 <https://doi.org/10.1056/NEJMc2103916>.
- [30] J.E. Ebinger, J. Fert-Bober, I. Printsev, M. Wu, N. Sun, J.C. Prostko, E.C. Frias, J.L. Stewart, J.E. Van Eyk, J.G. Braun, S. Cheng, K. Sobhani, Antibody responses to the BNT162b2 mRNA vaccine in individuals previously infected with SARS-CoV-2, *Nat. Med.* (2021).
522 <https://doi.org/10.1038/s41591-021-01325-6>.
- [31] X. Chi, R. Yan, J. Zhang, G. Zhang, Y. Zhang, M. Hao, Z. Zhang, P. Fan, Y. Dong, Y. Yang, Z. Chen, Y. Guo, J. Zhang, Y. Li, X. Song, Y. Chen, L. Xia, L. Fu, L. Hou, J. Xu, C. Yu, J. Li, Q. Zhou, W. Chen, A neutralizing human antibody binds to the N-terminal domain of the Spike protein of SARS-CoV-2, *Science*. (2020) eabc6952.
527 <https://doi.org/10.1126/science.abc6952>.
- [32] L. Liu, P. Wang, M.S. Nair, J. Yu, M. Rapp, Q. Wang, Y. Luo, J.F.-W. Chan, V. Sahi, A. Figueroa, X.V. Guo, G. Cerutti, J. Bimela, J. Gorman, T. Zhou, Z. Chen, K.-Y. Yuen, P.D. Kwong, J.G. Sodroski, M.T. Yin, Z. Sheng, Y. Huang, L. Shapiro, D.D. Ho, Potent neutralizing antibodies against multiple epitopes on SARS-CoV-2 spike, *Nature*. 584 (2020) 450–456.
532 <https://doi.org/10.1038/s41586-020-2571-7>.
- [33] Y. Cai, J. Zhang, T. Xiao, H. Peng, S.M. Sterling, R.M. Walsh, S. Rawson, S. Rits-Volloch, B. Chen, Distinct conformational states of SARS-CoV-2 spike protein, *Science*. (2020) eabd4251. <https://doi.org/10.1126/science.abd4251>.
- 536
537

538

539

540

541